Effect of sand dilation on core expansion during steel casting

D Galles and C Beckermann[1]
Department of Mechanical and Industrial Engineering, University of Iowa

E-mail: becker@engineering.uiowa.edu

Abstract. The thermo-mechanical behavior of the bonded sand used for molds and cores has a strong effect on dimensions of steel castings. Experiments are conducted in which a thick-walled hollow carbon steel cylinder is cast using a silica sand core. The temporal evolution of the inner diameter of the cylinder is measured in-situ during solidification and cooling by utilizing quartz rods connected to LVDTs (Linear Variable Differential Transformers). It is found that the inner diameter increases significantly during the initial stages of solidification when the steel offers little restraint to core expansion. Without accurately modeling this initial core expansion, the final cylinder dimensions at room temperature cannot be predicted. Preliminary simulations using the measured linear thermal expansion coefficient of the core considerably under-predict the measurements, which suggests that shear induced sand dilation also contributes to core expansion. The Drucker-Prager Cap model, which can predict dilative behavior, is used to simulate the mechanical behavior of the core. Utilizing this model in conjunction with an elasto-visco-plastic constitutive law for the steel, the stress simulations successfully predict the observed dimensional changes in the casting during solidification.

Introduction

During pattern design for steel sand castings, dimensional changes are estimated by specifying pattern allowances (PA [%] = {(pattern feature size – casting feature size)/ casting feature size} × 100). Several physical phenomena contribute to pattern allowances. Thermal contraction of the steel reduces unconstrained linear dimensions by approximately 2.2%. The sand mold and, specifically, cores impact dimensions in two ways. First, cores restrain the casting from free shrink to generate distortions (i.e., plastic strains). Second, cores expand into the mold cavity to reduce casting dimensions while the solidifying steel is weak and offers little restraint.

While the aforementioned mold effects have been previously investigated [1], an additional phenomenon that can also affect pattern allowances is sand dilation, i.e., volumetric expansion of a granular material due to a shear force. This behavior is illustrated in figure 1; in the undisturbed state, the sand grains are tightly-packed and contain small air voids between the grains (figure 1(a)). After a shear force is applied, however, the irregularly-shaped sand grains translate and/or rotate, causing the voids to grow, resulting in expansion of the sand aggregate (figure 1(b)).

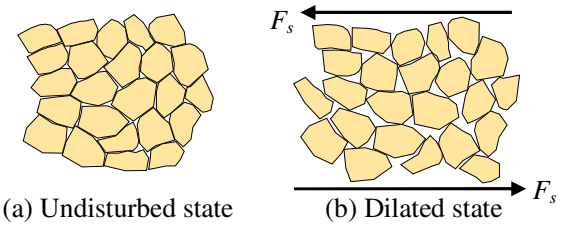

Figure 1. Sand dilation. (a) The undisturbed state of densely-packed sand. After a shear force, F_s, is applied, the voids between sand grains increase, resulting in dilation (i.e., volumetric expansion of the sand aggregate), as shown by the (b) dilated state.

Dilation is well-known within the geological community but has received little attention in the foundry industry and therefore, has (to the authors' best knowledge) not been considered as a significant contributor to pattern allowances. The purpose of this study is to measure the evolution of a casting feature during solidification in order to determine the effect of sand dilation. The results will then be used to validate a stress model employing the Drucker-Prager Cap (DPC) constitutive law, a pressure-dependent model capable of predicting dilative behavior.

For the experiments, a hollow carbon steel cylinder with a core is produced; the inner diameter of the cylinder is continuously measured in-situ with LVDTs. Thermocouples are utilized to record the temperature in the casting and at several locations in the core. For the simulations, a one-way temperature-displacement coupling is adopted; the transient temperature fields are solved first using commercial casting simulation software (MAGMASOFT® [2]). The results are then exported to a general purpose finite element stress analysis code (ABAQUS® [3]) to predict dimensional changes throughout the casting. By comparing the in-situ measurements to the predicted strains in the core and casting, sand dilation is quantified and predicted.

Description of experiments

1.1. Experimental setup and casting procedure

The casting geometry consisted of a hollow thick-walled cylinder with dimensions (in mm) shown in figure 2(a). The experimental setup is depicted in figure 2(b). The outer dimensions of the cope (280 mm length × 280 mm width × 75 mm height) and drag (280×280×200) are not drawn to scale. The change in the inner diameter at the mid-height of the cylinder was continuously measured by utilizing two identical assemblies consisting of a quartz rod, quartz tube, and LVDT. One end of the quartz rod was flattened into a disc (7 mm in diameter) using an oxy-acetylene torch and inserted through pre-drilled holes in the drag and core. The disc was butted to the outer diameter of the core, as shown in figure 2(b). In order to transmit displacement, the quartz rod passed through a quartz tube, which traversed the mold cavity. The other end of the quartz rod was attached to an LVDT, which continuously measured the displacement from one side of the inner diameter. The other assembly measured displacement on the opposite side of the cylinder. The LVDT measurements were added together to calculate the temporal evolution of the inner diameter. It is obvious from figure 2(b) that both LVDT measurements could not be taken at the same height. Therefore, one measurement was taken approximately 5 mm above the cylinder mid-height, while the other was taken 5 mm below.

Temperatures were measured at several locations; type K thermocouples were inserted through the bottom of the drag and into the core at radial distances of 6, 9, 15, and 25 mm from the vertical core-casting interface. Also, the thermocouples were staggered circumferentially to minimize the influence from other thermocouples. Finally, a type B thermocouple was encased in a quartz tube and inserted into the mold cavity to measure the temperature of the steel.

To build the molds, Unimin® IC55 silica lake sand was bonded with a phenolic urethane no-bake (PUNB) binder system. The binder (1.25% of mold weight) was mixed using a 55:45 ratio of part 1 (PEPSET® 1000) to part 2 (Techniset® 6435). The cope and drag were hand packed, whereas the cores were manually rammed. The core weights varied less than 2% among all experiments.

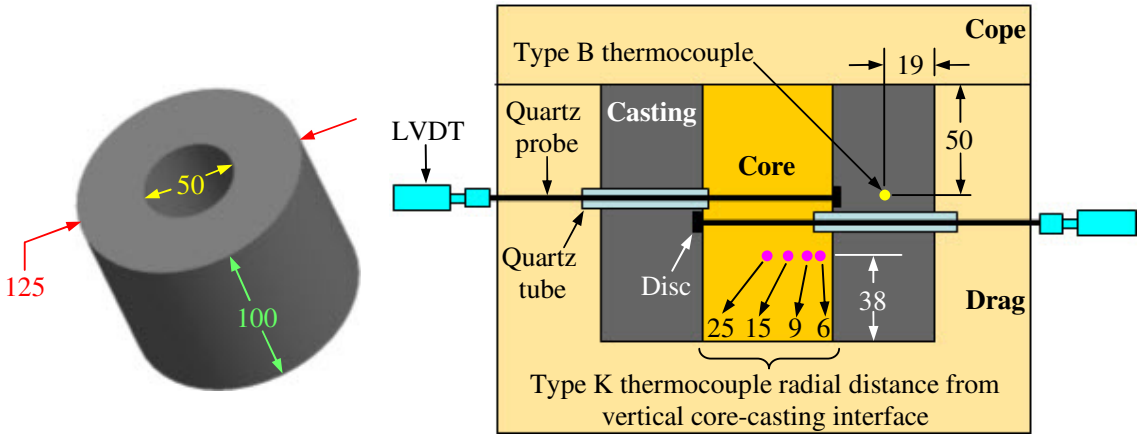

(a) Casting geometry (b) Experimental setup

Figure 2. (a) The casting geometry and (b) experimental setup at the casting mid-plane. Units in mm.

The steel was melted in a 300 lb induction furnace at the University of Northern Iowa Metal Casting Center. The target chemistry was ASTM A216 grade WCB carbon steel. Instead of using a pouring cup, liquid metal was poured directly into the mold cavity, after which the cope was placed on top of the drag. This methodology was chosen to eliminate mechanical interactions between the casting and the outer mold. In total, 5 castings were produced. For the first 4 castings, LVDT measurements and temperatures in the steel and the "25" location in the core (see figure 2(b)) were taken. For the 5th casting, no LVDT measurements were taken; only temperatures were recorded in the steel and at all core locations in figure 2(b).

1.2. Experimental Results

The changes in the inner diameter measured by the LVDTs (termed "LVDT measured") are plotted in figure 3 on (a) complete (40000 s) and (b) 600 s time scales. Figure 3(b) shows that the inner diameter expands to a maximum value (ranging from 1.15 mm in Cylinder 2 to 1.3 mm in Cylinder 1) at 200 s. This expansion occurs during solidification while the steel was mostly liquid and offered little restraint. After 200 s, the inner diameter remained constant until approximately 300 s, at which time solidification neared completion. After 325 s, the inner diameter decreases due to thermal contraction of the solid steel. The "wiggle" in the displacement curves seen at 4000 s in figure 3(a) can be attributed to a volumetric expansion associated with a solid-state phase transformation in the steel.

In addition to the LVDT measurements, pattern allowances were measured after shakeout at the three inner diameter locations indicated in figure 4(a). The results are shown in figure 4(b). The actual core dimensions (rather than pattern dimensions) were used to calculate pattern allowances to remove any variability due to the molding process. Measurements on the casting and core were taken with digital calipers. The dashed horizontal line in figure 4(b) denotes the free shrink of the steel (2.2%) and serves as a reference; any deviation from this line represents the core's contribution to dimensional changes. The largest deviation can be observed at the mid-height, while smaller deviations can be seen at the top and bottom. As a result, the inner surface of the cylinder evolved into a barrel-shaped profile. The variation in the pattern allowances with height can be explained by the local solidification times. When the steel solidifies more quickly, the impact of the core on dimensional changes is less and the resulting pattern allowance is closer to the free shrink line. This is the case at the top and bottom of the cylinder. At mid-height, the steel solidifies more slowly, core expansion occurs over a longer time, and the pattern allowance is farther away from the free shrink line. Another observation from figure 4(b) is that ID_{top} contained more scatter than the pattern allowances at the other locations, which can be explained by the manner in which the castings were

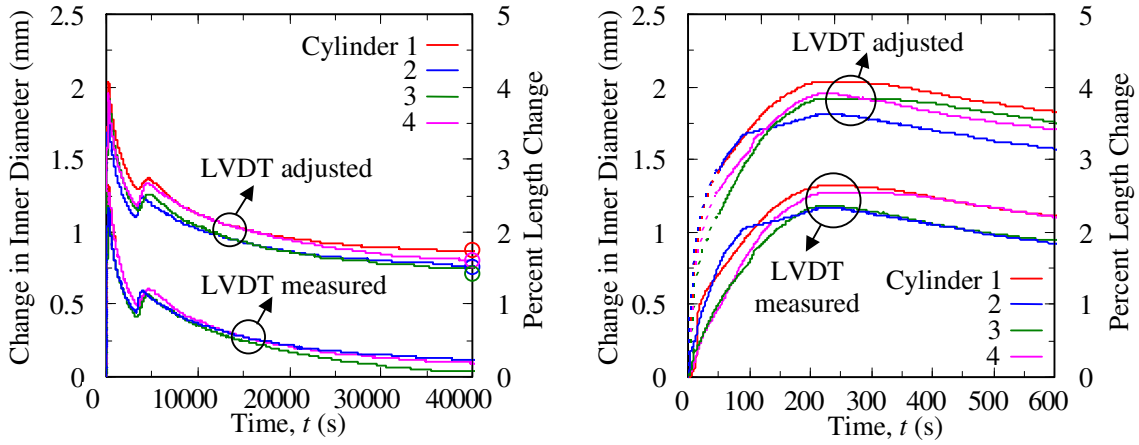

(a) Complete time scale (b) Initial 600 s

Figure 3. Measured change in inner diameter plotted on (a) complete and (b) 600 s time scales. The symbols on the secondary vertical axis on the complete time scale correspond to the pattern allowances at ID_{mid} in figure 4 and serve as the basis for shifting the measured curves upward.

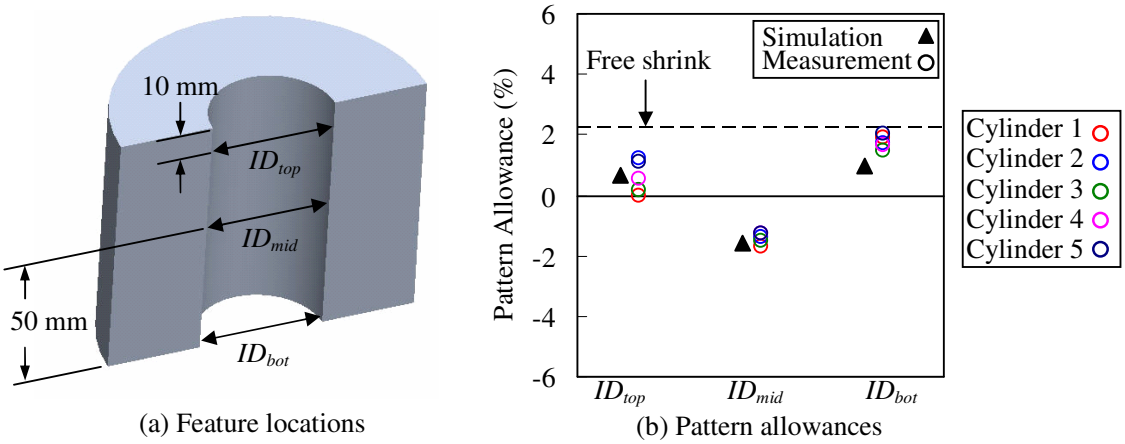

(a) Feature locations (b) Pattern allowances

Figure 4. Pattern Allowances. (a) Feature locations. (b) Measured and simulated pattern allowances.

poured. To avoid spilling steel onto the foundry floor, the mold was filled within a few mm from the top, leaving an air gap between the casting and cope. The variation in air gap thicknesses between the experiments likely affected local solidification times, which in turn influenced the pattern allowances at the top.

From figures 2(b) and 4(a), it can be seen that ID_{mid} is the same feature that was measured by the LVDTs. Therefore, the percent change of the inner diameter at room temperature in figure 3(a) should match the negative pattern allowance of ID_{mid}. Unfortunately, this is not the case, as a maximum expansion of 0.27% at room temperature was measured by the LVDTs, whereas the negative pattern allowances at ID_{mid} were about 1.75%. Hence, approximately 1.5% (0.75 mm) additional core expansion was measured by the calipers over the LVDTs. This discrepancy can be attributed to the LVDT measurements. As confirmed below by the stress simulations, the thermal contraction of the steel after 325 s is accurately measured by the LVDTs. Therefore, the discrepancy between the LVDT measurements and pattern allowances originated from the LVDTs during the initial 325 s. During these early times, the steel adjacent to the core at mid-height existed in a liquid or semi-solid state, which resulted in slippage between the quartz probes and the steel. In order to account for this

slippage, the entire LVDT curves in figure 3 were shifted upward to match the measured pattern allowance at room temperature (40,000 s). The negative pattern allowances are shown as open circles on the secondary (right) vertical axis in figure 3(a). Then, the LVDT curves were modified during the initial 50 s to smoothly increase from zero to the shifted measurements. These modifications are shown as dashed lines in figure 3(b). The resulting curves are termed "LVDT adjusted" and will be used below to validate the stress model predictions.

Thermal simulations

Thermal simulations of the casting process were performed using MAGMASOFT®, a detailed description of which can be found elsewhere [4]. Excellent agreement between measured and predicted temperatures was achieved at all times, as shown by the temperature vs. time plots on complete and 600 s time scales in figures 5(a) and 5(b), respectively. The predicted transient temperature fields were subsequently transferred to the finite element mesh used in the stress simulations.

Stress Simulations

Stress simulations were performed with ABAQUS®. Only the casting and core were simulated, as the outer mold had minimal impact on the inner diameter evolution. For preliminary simulations, only thermal strains were calculated in the core and cylinder. These simulations are important for two reasons. First, if the predicted thermal expansion of the core under-predicts the measured inner diameter expansion (see figure 3(b)), then dilation of the core must indeed be significant. Second, if the predicted thermal strains in the cylinder match the LVDT results after 325 s, the method used to shift the LVDT curves in figure 3 is justified. Thermal strains were predicted using the linear thermal expansion (LTE) curves shown in figure 6. The steel LTE was calibrated in a previous study [4], with the onset of thermal contraction of the steel (1410°C) occurring at a solid fraction of 0.97. The LTE for bonded silica sand was measured with a dilatometer at the University of Northern Iowa. The strong expansion at 1470°C represents the transformation to cristobalite.

The predicted variations in the inner diameter of the steel cylinder at mid-height from the purely thermal strain simulation are plotted in figure 7. The inner diameter is predicted to begin contraction after 250 s. The predicted and measured curves are exactly parallel after 325 s, which confirms that the dimensional changes measured by the LVDTs after 325 s were indeed solely due to thermal contraction of the steel. Hence, the method used to shift the measured LVDT curves in figure 3 is justified.

The outer diameter of the core at mid-height is predicted by the purely thermal strain simulations to increase to a maximum value of 0.5 mm at about 150 s (see figure 7(b)). Subsequently, the diameter increases marginally until 6,000 s (due to the decreasing sand LTE between 600°C and 1470°C in figure 6), after which it decreases as the core cools to room temperature. The maximum expansion of the core at 150 s (0.5 mm) is far less than the measured maximum "LVDT adjusted" value of 1.9 mm. Therefore, 1.4 mm of expansion cannot be explained by thermal strains in the core. This suggests that dilation of the core indeed plays an important role in determining the dimensional changes of the casting. One caveat that would create additional thermal expansion is cristobalite formation, which was not predicted by the simulations. This is because the maximum predicted core temperature (i.e., the interface value at 200 s in figure 5(b)) was lower than the transformation temperature of 1470°C. However, impurities in the sand mold are known to reduce the temperature at which cristobalite forms. Hence, an additional experiment was performed, in which layers of sand were extracted in 1 mm increments from the mold-metal interface from a steel casting after it cooled to room temperature. Because the cristobalite transformation process is essentially irreversible [5], any cristobalite formed at high temperatures also remains at room temperature. The sand samples were tested using x-ray diffraction, from which minimal amounts of cristobalite were detected. Therefore, expansion due to cristobalite formation can be excluded as a reason for the observed core expansion.

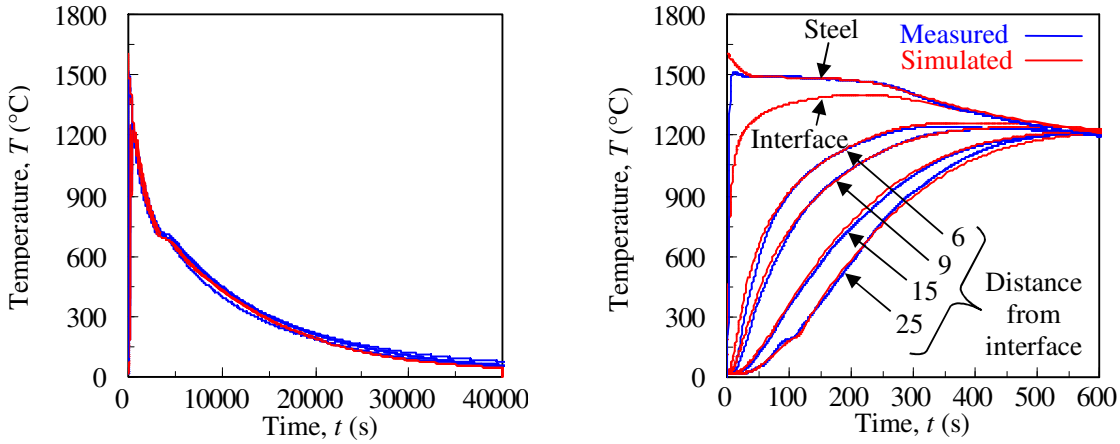

(a) Complete time scale (b) Initial 600 s

Figure 5. Comparison between measured and predicted temperatures in the steel and throughout the core on (a) complete and (b) 600 s time scales.

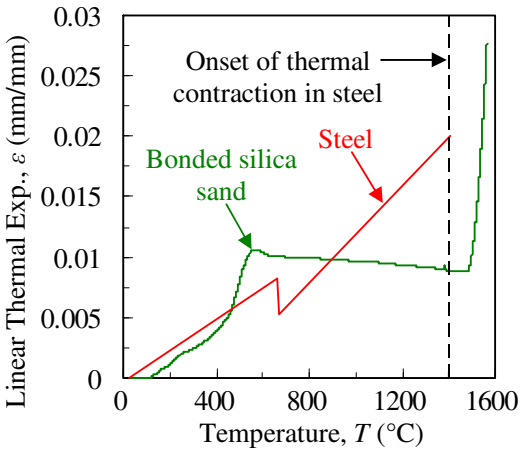

Figure 6. Linear thermal expansion (LTE) for the steel and bonded silica sand. The onset of thermal contraction in the steel (1410°C) corresponds to a solid volume fraction of 0.97.

After the preliminary simulations, full stress simulations were performed using an elasto-visco-plastic constitutive law (implemented in a user-defined UMAT subroutine) for the steel and the Drucker-Prager Cap (DPC) model for the core. Features of the elasto-visco-plastic model include rate, hardening, and temperature effects, as well as pressure-dependent deformation during solidification. The complete model, including the calibration of its parameters, is described elsewhere [4]. The preliminary simulations showed that negligible viscoplastic strains are generated after solidification, which implies the simulations are insensitive to changes in the viscoplastic parameters. However, one parameter that requires consideration is the coherency solid fraction, g_{coh}, which defines the solid fraction at which the steel can transmit stresses. For the current study, g_{coh} = 0.75 was specified. Any g_{coh} lower than this value generated insufficient core expansion.

Figure 8 shows the DPC yield surface in q (shear stress) vs. p (pressure) space. The critical feature of the DPC model for the present study is the ability to predict dilation, which occurs during yielding on the shear failure surface, F_s. Other features of the model include a pressure-dependent yield surface containing a cap, F_c, which prevents dilation at high pressures. The transition yield surface, F_t (defined by parameter α), provides a smooth transition between F_s and F_c to avoid numerical issues. The compressive strength of the material, p_b, defines the position of the cap on the pressure axis. A detailed explanation of the model can be found in a suitable plasticity textbook.

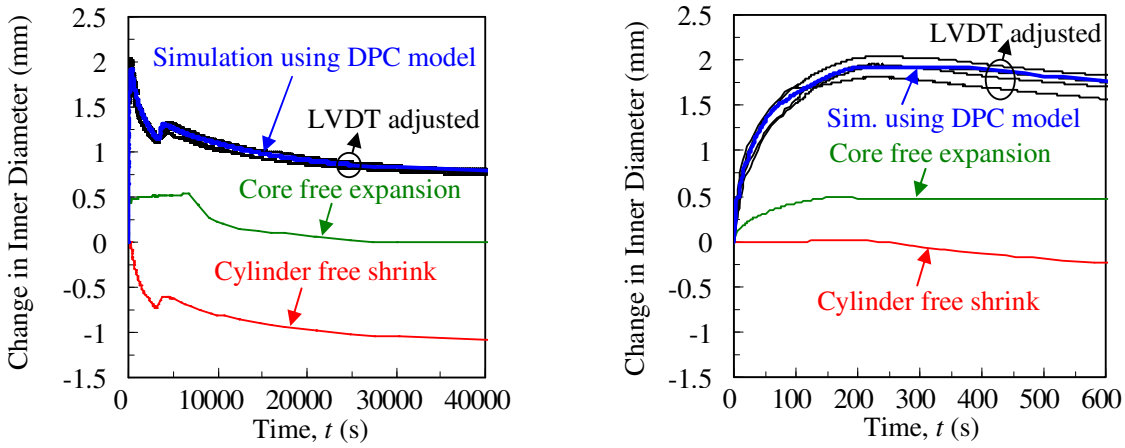

(a) Complete time scale (b) Initial 600 s

Figure 7. Comparison between measured and predicted inner diameter temporal evolutions on (a) complete and (b) 600 s time scales.

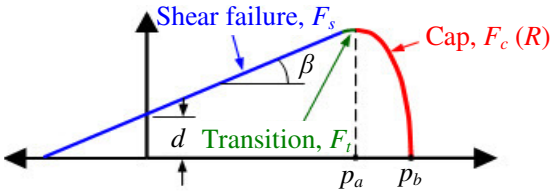

Figure 8. The Drucker-Prager Cap (DPC) yield surface is defined by the shear failure (F_s), cap (F_c), and transition (F_t) surfaces. Dilation is predicted when yielding occurs on F_s.

The mechanical properties of the sand core were estimated as follows. At temperatures less than 180°C, the modulus of elasticity (E) and cohesion (d) were taken from tests on PUNB bonded sand [6]. After the binder pyrolyzes (≈ 200°C), experimental stress-strain data for dense sand at room temperature [7-9] were used as a first estimate to determine the high-temperature DPC model parameters. Elastic properties (E and v) were taken from [7]. Hardening measurements of Lade et al. [8] were used to determine p_b. The cohesion (d), friction angle (β), and cap eccentricity (R) were estimated from data in Hettler and Vardoulakis [9]. At 25°C and 180°C, the larger cohesion values required either an increase in p_b or decrease in R. A parametric study found neither to have an impact on predicted dimensions for this study. Therefore, R was decreased to a small value at these temperatures. The final DPC model parameters are summarized in table 1. Initially, the stress simulations predicted excessive core expansion. To match the measured and predicted inner diameter evolutions (see below), the cohesion was increased from 0.025 to 0.05 MPa. This increase is not unexpected, as chemical reactions during binder decomposition will likely increase the strength [6].

Table 1. Parameters used in Drucker-Prager Cap Model

T (°C)	β (degrees)	d (MPa)	R	α	p_b (MPa)	E (MPa)	v
25	37.6	1.8	0.01	0.01	5	3403	0.3
180	37.6	0.2	0.01	0.01	5	282	0.3
> 300	37.6	0.05	0.85	0.01	5	61	0.3

Figure 7 shows that using the DPC model excellent agreement between the measured and predicted time evolutions of the inner diameter at mid-height is obtained. In particular, the early expansion of the core by 1.9 mm is predicted correctly. As shown in figure 4(b), the pattern allowances are predicted well not only at mid-height, but also at the top and bottom of the cylinder. The predicted barrel-shaped profile of the core can be clearly observed in figure 9. The von Mises stresses and pressures at 150 s are also plotted in figure 9. The von Mises stresses in the core range from 50 kPa to 400 kPa. They are induced by the uneven heating of the core and the non-uniform solidification and contraction of the steel around it. Recall that the existence of these shear stresses is essential for the prediction of dilation.

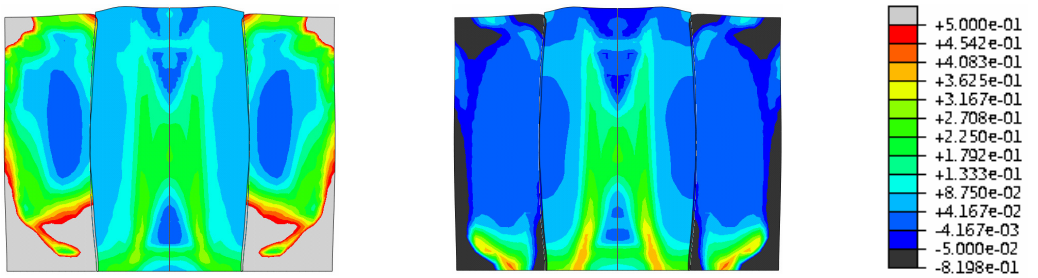

(a) von Mises stress (b) Pressure

Figure 9. (a) von Mises stress and (b) pressure at 150 s. Units in MPa. Deformation factor = 5.

Conclusion

In this study, the effect of sand dilation on core expansion during steel casting was studied through experiments and stress simulations. The inner diameter evolution of a thick-walled hollow steel cylinder was measured in-situ with LVDTs during casting. It was found that the measured expansion of the inner diameter far exceeded the predicted thermal expansion of the core. To account for this additional expansion, core dilation was considered. In order to model dilation, the Drucker-Prager Cap (DPC) model was utilized in the stress simulations. The simulation successfully predicted the measured evolution of the inner diameter. The measured pattern allowances revealed a barrel-shaped profile of the inner diameter, which was also predicted by the simulations. This study sheds considerable light on the physical phenomena responsible for dimensional changes during casting of steel and the resulting pattern allowances. Dilation of the mold or core sand, in addition to thermal expansion, can play a significant role during early times, when the steel offers little resistance to deformation. The stress simulations in this study are preliminary in that the material parameters for the DPC model, in particular at high temperatures, were only estimated from room temperature sand data.

References

[1] Peters F, Voight R, Ou S Z and Beckermann C 2007 *Int. J. Cast Metals Res.* **20** 275-87
[2] ABAQUS®, Abaqus, Inc., Providence, RI
[3] MAGMASOFT® v4.6, Magma GmbH, Aachen, Germany
[4] Galles D and Beckermann C 2013 *67th SFSA Technical and Operating Conf.* (Chicago, IL)
[5] Carniglia S C 1992 *Handbook of Industrial Refractories Technology* (Park Ridge, NJ) Noyes Pub
[6] Thole J and Beckermann C 2010 *Int J Metalcasting* **4** 7-18
[7] Brown P T 1995 *Geotechnical Testing J.* **18** 259-70
[8] Lade P V, Yamamuro J A and Bopp P A 2006 Geomechanics II: Testing, Modeling, and Simulation ed P V Lade and T Nakai pp 87-102
[9] Hettler A and Vardoulakis I 1984 *Geotechnique* **34** 183-98

Acknowledgements

This research is sponsored through the Defense Logistics Agency through the American Metalcasting Consortium and the Steel Founders' Society of America.